

# Smooth Vertical Surface Climbing With Directional Adhesion

Sangbae Kim, *Student Member, IEEE*, Matthew Spenko, *Member, IEEE*, Salomon Trujillo, Barrett Heyneman, Daniel Santos, *Student Member, IEEE*, and Mark R. Cutkosky, *Member, IEEE*

**Abstract**—Stickybot is a bioinspired robot that climbs smooth vertical surfaces such as glass, plastic, and ceramic tile at 4 cm/s. The robot employs several design principles adapted from the gecko including a hierarchy of compliant structures, directional adhesion, and control of tangential contact forces to achieve control of adhesion. We describe the design and fabrication methods used to create underactuated, multimaterial structures that conform to surfaces over a range of length scales from centimeters to micrometers. At the finest scale, the undersides of Stickybot’s toes are covered with arrays of small, angled polymer stalks. Like the directional adhesive structures used by geckos, they readily adhere when pulled tangentially from the tips of the toes toward the ankles; when pulled in the opposite direction, they release. Working in combination with the compliant structures and directional adhesion is a force control strategy that balances forces among the feet and promotes smooth attachment and detachment of the toes.

**Index Terms**—Bioinspired, climbing robot, dry adhesive, gecko-inspired, legged robot, mobile robot, under-actuated.

## I. INTRODUCTION

MOBILE robots that can climb and maneuver on vertical surfaces are useful for inspection, surveillance, and disaster relief applications. Previous robots capable of climbing exterior building surfaces such as stucco and brick have utilized microspines similar to those found on insects [2], [29] or a controlled vortex that creates negative aerodynamic lift [32]. Smooth vertical surfaces have been climbed using suction [24], [38], magnets [8], [34], and pressure-sensitive adhesives (PSAs), such as tape [13], [31]. PSAs exhibit high adhesion on smooth surfaces but foul easily and require relatively high

Manuscript received January 31, 2007. This paper was recommended for publication by Associate Editor P. Dario and Editor F. Park upon evaluation of the reviewers’ comments. This work was supported by the DARPA BioDynamics Program. The work of M. Spenko was supported by the Intelligence Community Postdoctoral Fellow Program. The work of D. Santos was supported by the Stanford-NIH Biotechnology Training Grant. Some material in this paper has been adapted from two papers, [23], [28], presented at the IEEE ICRA 2007.

S. Kim, S. Trujillo, B. Heyneman, D. Santos, and M. R. Cutkosky are with the Center for Design Research, Stanford University, Stanford, CA 94305-2232 USA (e-mail: sangbae@stanford.edu; sjtrujil@stanford.edu; heyneman@stanford.edu; dsantos@stanford.edu; cutkosky@stanford.edu).

M. Spenko is with Illinois Institute of Technology, Chicago, IL 60616-3793 USA (e-mail: mspenko@iit.edu).

This paper has supplementary downloadable multimedia material available at <http://ieeexplore.ieee.org>, provided by the author. This material includes one video (Stickybot\_IEEE.mov) Stickybot\_IEEE\_readme demonstrating Stickybot’s climbing capabilities showing climbing on smooth surfaces along with the description of detail design and Directional Adhesive that Stickybot uses, and it plays in Quick Time only (extension could be .mov). The size is 9 MB. Contact sangbae@stanford.edu or cutkosky@stanford.edu for further questions about this work.

Color versions of one or more of the figures in this paper are available online at <http://ieeexplore.ieee.org>.

Digital Object Identifier 10.1109/TRO.2007.909786

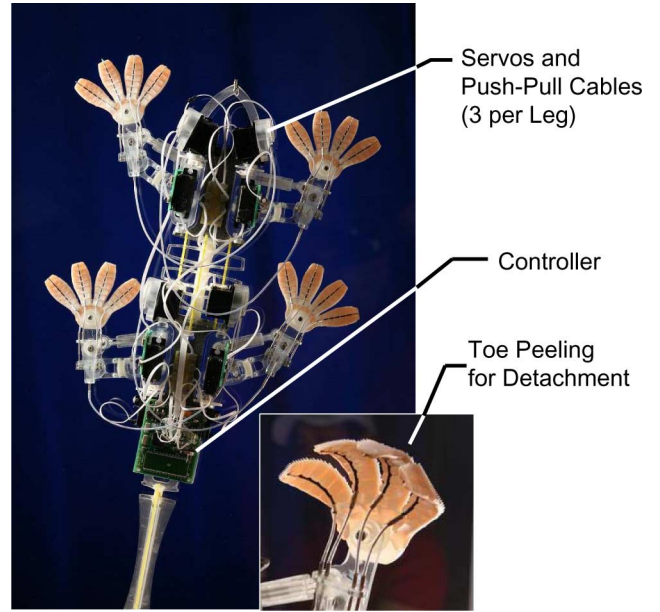


Fig. 1. Stickybot, a new bioinspired robot capable of climbing smooth surfaces. Inset: detail of toes curling to facilitate detachment.

forces for attachment and detachment. Some researchers have circumvented this problem by using spoked-wheel designs that allow the detachment force at a receding point of contact to provide the necessary attachment force at the next [13]. Wet adhesive materials have also been employed, drawing inspiration from tree frogs and snails [10]. All of these solutions have been successful, but are limited in their range of surfaces. To develop a robot capable of climbing a wide variety of materials, we have taken design principles adapted from geckos. The result is Stickybot (Fig. 1), a robot that climbs glass and other smooth surfaces using directional adhesive pads on its toes.

Geckos are arguably nature’s most agile smooth surface climbers. They can run at over 1 m/s, in any direction, over wet and dry surfaces of varying roughness and of almost any material, with only a few exceptions like graphite and Teflon [3]. The gecko’s prowess is due to a combination of “design features” that work together to permit rapid, smooth locomotion. Foremost among these features is hierarchical compliance, which helps the gecko conform to rough and undulating surfaces over multiple length scales. The result of this conformability is that the gecko achieves intimate contact with surfaces so that van der Waals forces produce sufficient adhesion for climbing [3].

The gecko’s adhesion is also directional. This characteristic allows the gecko to adhere with negligible preload in the

normal direction and to detach with very little pull-off force, an effect that is enhanced by peeling the toes in “digital hyperextension” [4].

A consequence of the gecko’s directional adhesion is that it must control the orientation of its feet when ascending or descending. In addition, the gecko controls the tangential contact forces to achieve smooth climbing with minimal pull-off forces [5].

In the following sections, we examine hierarchical compliance, directional adhesion, and force control for climbing in more detail, and describe how they are implemented in Stickybot. We also provide details of the design and fabrication of Stickybot’s feet equipped with arrays of directional polymer stalks (DPS). We present the results of experiments to confirm the DPS directional behavior and describe the controller used to ensure that they are loaded appropriately. We also present a comparison of attachment and detachment forces for Stickybot climbing with directional versus nondirectional adhesives, illustrating the advantages of the former. We conclude with a discussion of some of the limitations of the current Stickybot technology and plans to overcome them for faster, more robust, and more dirt-tolerant climbing in the future.

## II. ADHESION AND COMPLIANCE

When two surfaces are brought together, adhesion is created via van der Waals forces. Since van der Waals forces scale as  $1/d^3$ , where  $d$  is the local separation between two flat surfaces [17], it is critical for the surfaces to be within an order of 10 s of nanometers of each other. PSAs accomplish this with a soft layer that flows and conforms to the surface, thus maximizing the contact area. PSAs can provide sufficient adhesion levels for a robot to climb a wall [13], [31], but they have several disadvantages compared to the hierarchical compliant structures used by geckos. To adhere to rough surfaces, an additional layer of conformability is usually required, which is why high-performance adhesive tapes for relatively rough surfaces often have a backing layer of soft foam [27]. Substantial preloads in the normal direction are required to achieve adhesion, and large forces are also required for detachment, leading to inefficient climbing. In addition, PSAs quickly become contaminated with dirt and lose their stickiness.

To overcome the limitations of PSAs, there has been recent interest in creating synthetic “dry” or “self-cleaning” adhesives that do not foul over time. These adhesives use stiff, initially nonsticky bulk materials in combination with microstructured geometries to conform to surfaces. Fig. 2 shows some adhesive solutions ordered in terms of feature size, effective modulus, and general trend of shape sensitivity based on size. For a material to be considered tacky, its effective modulus must be less than 100 kPa [3], [6], [11]. This “tack criterion” comes from the need to conform intimately to a surface in order for van der Waals forces to become significant. The gecko conforms to surfaces despite having a relatively high bulk material stiffness ( $\approx 2$  GPa for  $\beta$ -keratin) [3] by using a hierarchy of microstructures consisting of lamellae, setae, and spatulae. This hierarchical geometry lowers the effective stiffness of whole structure to

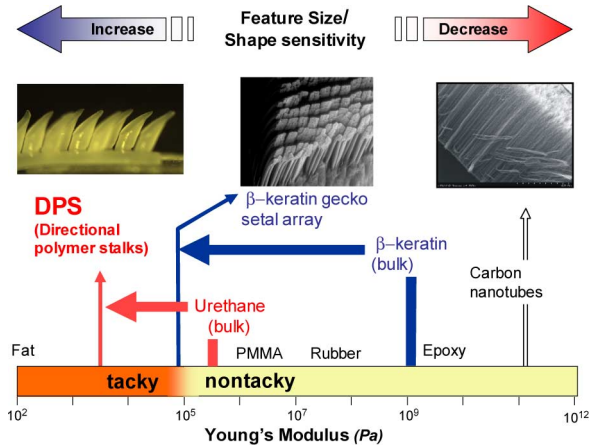


Fig. 2. Modulus of bulk material and feature size of distal end of different structures. Microstructured geometries can lower the overall stiffness of bulk materials so that they become tacky. This principle allows geckos to use  $\beta$ -keratin for their adhesive structures. In smaller scale, tip geometry plays less important role in adhesion forces, at given bulk material modulus.

make the system function like a tacky material without causing fouling. Fibrillar structure also helps force distribution by splitting contact surfaces.

Several types of synthetic dry adhesives have been manufactured, including arrays of vertically oriented multiwall carbon nanotubes [36], [37] and polymer fibers [16], [21], [25], [30]. These adhesives use stiff, hydrophobic materials, and have achieved useful levels of adhesion, but only with careful surface preparation and high normal preloads.

An alternative method to creating adhesives is to start with a somewhat softer material on the order of 300 kPa to 3 MPa. These materials can employ larger feature sizes and still conform to surfaces because they are softer to begin with. Unlike dry adhesives, these materials will attract dirt; however, in contrast to PSAs, they can be cleaned and reused. One such example is a microstructured elastomer tape [12], [26].

In addition to effective stiffness of corresponding structure, the size and shape of the contacting elements is important in sustaining adhesion [1], [14]–[16], [22], [35]. At given loading direction, having special tip geometry is beneficial to reduce stress concentration increasing adhesion of a single distal element (i.e., spatular of gecko). Interestingly, in smaller scale, tip geometry is less important than in bigger scale since it requires less deformation energy that induces better stress distribution across the contact surface. Therefore, for smaller size, sensitivity to tip geometry is relatively low, but for larger features, tip geometry dramatically affects adhesion at constant bulk material stiffness. Fig. 2 (top) shows general tendency of shape sensitivity. The arrows from three different examples indicate only the tip size regardless of their Young’s modulus. At relatively bigger tip sizes [ $O(100 \mu\text{m})$ ], the optimal tip geometry, where stress is uniformly distributed along the contact area, has a theoretical pull-off force of more than 50–100 times that of a poor tip geometry [14]. Softer material for the tip reduces deformation energy and decrease shape sensitivity but increases chances of fouling and clumping. In order to achieve balance among prevention of fouling and clumping,

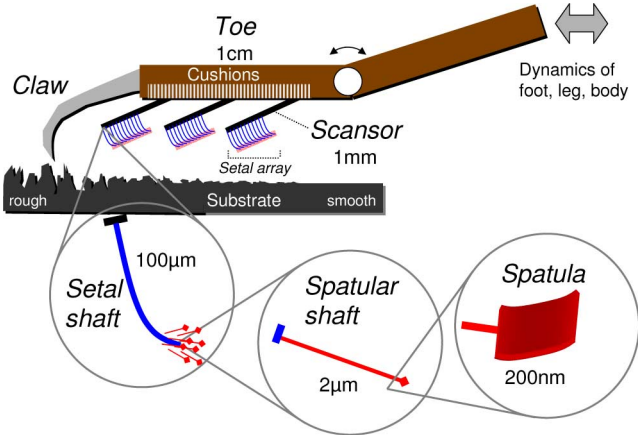


Fig. 3. Hierarchy of compliant structures in the gecko for conforming at many length scales. (From [6], reprinted with the permission of K. Autumn).

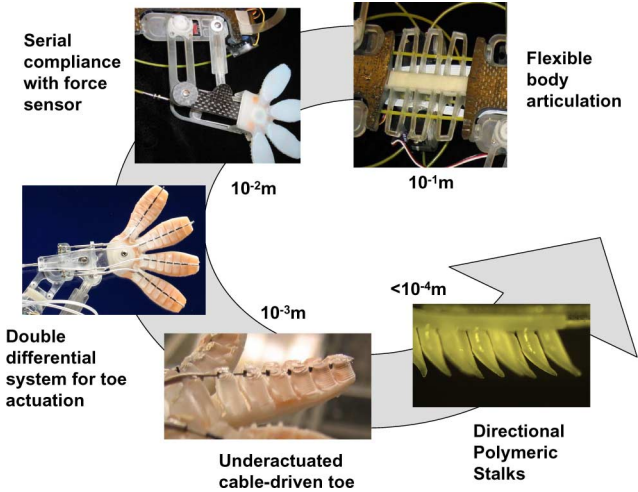


Fig. 4. Elements of Stickybot's hierarchical compliance over a range of length scales.

soft effective stiffness, low shape sensitivity, and somewhat wider working range of loading condition, it is advantageous to have smaller tip. This might help us to understand why nature evolution decided to use nano scale structure for adhesion system.

#### A. Hierarchical Conformability in the Gecko

For climbing rough surfaces such as cave walls and trees, many levels of conformability are required. In the gecko, the flex of the body and limbs allows for conformation at the centimeter scale. The body presses flat against curved surfaces to reduce the pull-in forces needed to prevent pitching back. At the scale of a several millimeters, the toes conform independently to local surface variations. The bottom surfaces of toes are covered with lamellae that conform at the millimeter scale. The lamellae consist of arrays of setal stalks, as shown in Figs. 2 and 3. The consequence of the gecko's hierarchical system of compliances is that it can achieve levels of adhesion of over 500 kPa on a wide variety of surfaces from glass to rough rock, and can support its entire weight in shear from just one toe [7].

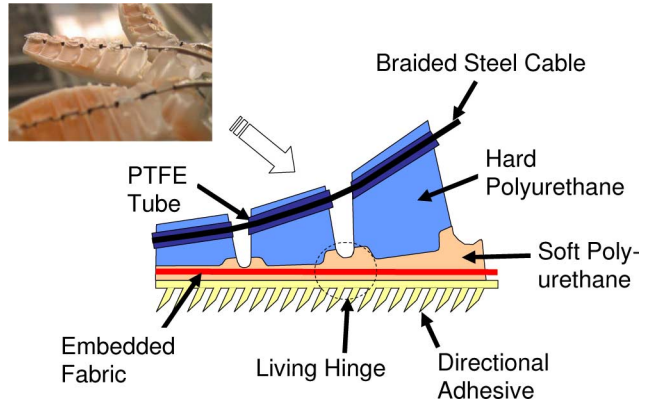


Fig. 5. Schematic of cross-section view of Stickybot toe fabricated via shape deposition manufacturing.

#### B. Hierarchical Conformability in Stickybot

Stickybot uses an analogous, albeit much less sophisticated, hierarchy of conformable structures to climb a variety of smooth surfaces (Fig. 4). At the body level, Stickybot has 12 servomotors and 32 degrees of freedom (DOFs), making it highly underactuated. The structures of the torso, legs, and feet are manufactured using shape deposition manufacturing [9], [33] with two grades of polyurethane (innovative polymers: 72 Shore-DC and 20 Shore-A hardness). The upper and lower torso and forelimbs are reinforced with carbon fiber, making them the strongest and stiffest components. The middle of the torso is designed as a compromise between sufficient compliance to conform to surfaces and sufficient stiffness so that normal forces of approximately  $\pm 1$  N can be applied at the feet without excessive body torsion.

The feet of Stickybot consist of four segmented toes molded with two grades of polyurethane that sandwich a thin polyester fabric (Fig. 5). The fabric flexes easily, but is relatively inextensible so that it transmits shear stresses across the surface of the foot to avoid the buildup of stress concentrations, and subsequent peeling, at the proximal regions of the toes.

The bending of the toes allows them to conform to gently curved surfaces ( $r \geq 5$  cm, where  $r$  is the radius of curvature), and to peel backward in a motion that approximates the digital hyperextension that geckos use to facilitate detachment. The action is created using a servomotor connected via push-pull cables in sleeves, attached to a rocker-bogie linkage located at the foot (Fig. 6).

The profile of the steel cable running along the topside of each toe is calculated to achieve a uniform stress distribution when the toes are deployed on a flat surface (Fig. 7). Assuming an approximately uniform toe width, the sum of the forces in the  $y$ -direction is given as

$$T \sin \theta - T \sin (\theta + \delta\theta) + F_N = 0 \quad (1)$$

where  $T$  is the force acting along the cable,  $\theta$  is the angle of the cable with respect to the horizontal, and  $F_N$  is the normal force acting on the bottom of the toe. To ensure uniform attachment of

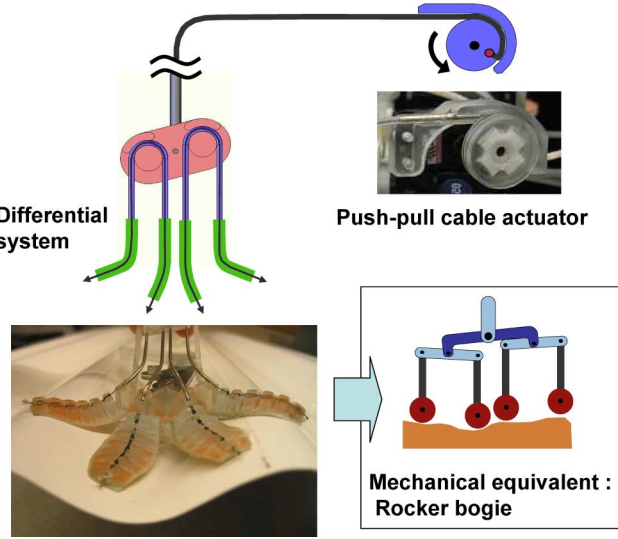


Fig. 6. Two-stage differential system actuated by a single push-pull actuator. It facilitates conformation on uneven surfaces and distributes the contact forces among four toes.

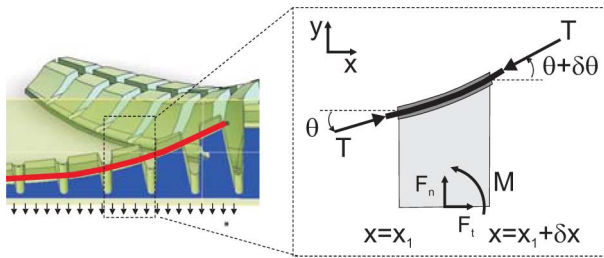


Fig. 7. Details of nomenclature used to calculate cable profile of the toes.

the foot, a constant pressure on the bottom of the toe is desired:

$$\frac{T(\sin(\theta + d\theta) - \sin \theta)}{dx} = \frac{F_N}{dx} = \sigma. \quad (2)$$

Expanding the term  $\sin(\theta + d\theta)$ , and assuming that  $d\theta$  is small such that  $\cos d\theta = 1$  and  $\sin d\theta = d\theta$  yields

$$\cos \theta d\theta = \frac{\sigma}{T} dx. \quad (3)$$

Integrating both sides and solving for  $\theta$  gives

$$\theta = \arcsin\left(\frac{\sigma x}{T}\right). \quad (4)$$

The slope of the cable profile is thus

$$\frac{dy}{dx} = \tan\left(\arcsin\left(\frac{\sigma x}{T}\right)\right). \quad (5)$$

Integrating with respect to  $x$  yields the profile of the cable

$$y(x) = -\frac{T}{\sigma} \sqrt{1 - \left(\frac{\sigma x}{T}\right)^2} \quad (6)$$

which is simply a circular arc with radius  $T/\sigma$ .

At the scale less than hundreds of micrometers, Stickybot conforms to the surface with synthetic adhesive patches (Fig. 5). Currently, the best results have been obtained using arrays of small, asymmetric features made out of polyurethane with a

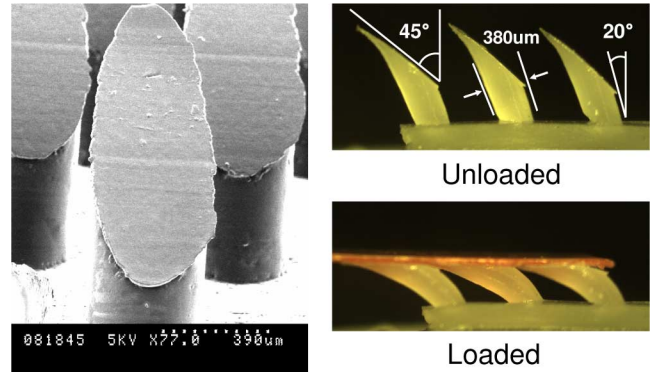


Fig. 8. Anisotropic hairs comprised 20 Shore-A polyurethane. Hairs measure  $380 \mu\text{m}$  in diameter at the base. The base angle is  $20^\circ$  and the tip angle is  $45^\circ$ .

modulus of elasticity of  $\approx 300$  kPa (Fig. 8). For climbing robots, higher adhesion in tangential direction loading is significant; therefore, the tip geometry need to be designed for the distribution of tangential load. This requirement limits the available size range where we can control the tip geometry. The bulk material modulus is chosen for soft normal effective stiffness and enough range of loading direction. A detailed description of directionality of the patches is given in the following section including the manufacturing process and importance of the anisotropic geometry. We are currently investigating alternate manufacturing methods that will yield finer feature sizes and comparable adhesion with stiffer materials.

### III. DIRECTIONAL FRICTION AND ADHESION

As discussed in [4], the gecko's toe structures are only adhesive when loaded in a particular direction. Moreover, the amount of adhesion sustained is a direct function of the applied tangential load. In other words, the gecko can control adhesion by controlling tangential forces. The anisotropic adhesion results from the gecko's lamellae, setae, and spatulae, all being angled instead of aligned vertically. Only by pulling in the proper direction does the gecko align its microstructures to make intimate contact with the surface.

DPSs were designed and manufactured to create an adhesive that is also directional like the gecko's system. DPS are made out of a soft polyurethane (innovative polymers, IE-20 AH polyurethane, 20 Shore-A hardness,  $E \approx 300$  kPa), and are shown in Fig. 8. The initial bulk material can be quite stiff because of the complexity of the gecko hierarchical system; however, DPS begin with a fairly soft material that is already marginally sticky. Geometric properties were determined empirically, drawing inspiration from the shapes of gecko setae. Not having fine distal structures like spatulae, the DPS need low-stiffness tips in order to make contact without high normal preload. The sharp and thin ( $<30 \mu\text{m}$ ) tip shape of DPS is designed to create a softer effective stiffness when pulled parallel to the angle of inclination.

The overall mold to create DPS consists of three parts. The middle mold is made out of delrin, which has good machinability and relatively low surface energy so that it does not

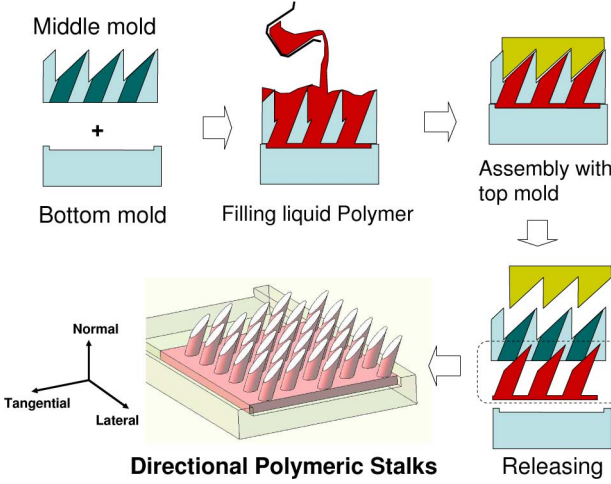


Fig. 9. Molding process used to fabricate anisotropic patches. Mold is manufactured out of hard wax and then filled with liquid urethane polymer. A cap eliminates contact with air and creates final tip geometry.

bond to the curing polymer. First, V-shaped grooves are made in a 1.6 mm-thick delrin sheet, as shown in Fig. 9. Before the drilling process, the top mold is fabricated by casting silicone rubber on the middle mold. On the 45° slanted surfaces and at a 20° tilted angle, 380  $\mu\text{m}$  holes are made in a hexagonal pattern, maximizing stalk density. The bottom mold is made out of a wax that has the Stickybot toe pattern.

Before pouring polymer, the middle and bottom mold are assembled. After pouring polymer on this assembly, the top mold is applied, squeezing out any excess material. The DPS array is released after curing by disassembling the molds. An alternative manufacturing method has also been used to create softer and smoother tip surfaces. Instead of using a top mold, excess polymer is simply wiped off of the 45° slanted surfaces, and the polymer is exposed to air during curing. Exposure to atmospheric moisture during the cure creates softer and stickier tips. However, this method is less desirable because it is difficult to control the moisture-induced softening. The wiping process is also labor intensive.

The DPSs were tested using a three-axis positioning stage and a six-axis (ATI Gamma Transducer) load cell in order to study their adhesive characteristics. The stage was able to control motion of the DPS in the normal, tangential (fore-aft), and lateral direction of the DPS (Fig. 9). The load cell was used to measure the pull-off force when the patches detached from a glass substrate. Patches of the DPS were brought into contact, preloaded, and then pulled away from the glass at different departure angles. When the patches are pulled in directions along the stalk angle, they exhibit moderate amounts of adhesion. When pulling in the opposite directions, adhesion disappears and Coulomb friction is observed.

Data from the tests are shown in Fig. 10 for the normal tangential plane, plotted in force space. Fig. 10 also shows the frictional adhesion model, which has been proposed in [4] as a simple way to describe the macroscopic gecko adhesion system, and the well-known isotropic Johnson–Kendall–Roberts (JKR) model for elastomers [18]. The JKR model provides a

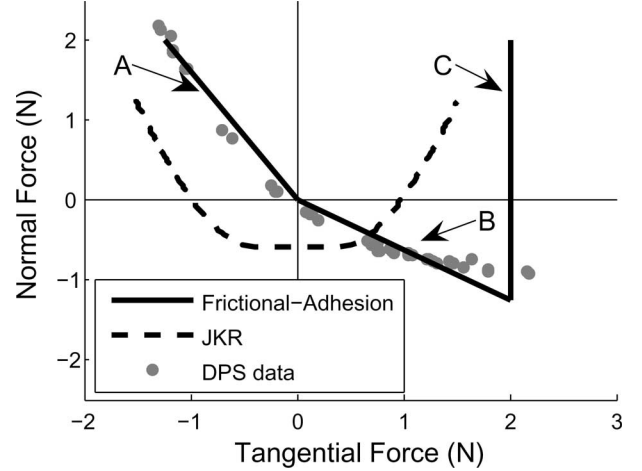


Fig. 10. Comparison of the frictional adhesion model [4] and the JKR model [18] with pull-off force data from a single toe of Stickybot's directional adhesive patches (513 stalks). (A) When dragged against the preferred direction, the directional patch exhibits friction and no adhesion. (B) When dragged in the preferred direction, the directional patch demonstrates adhesion proportional to the shear force, albeit with saturation at the highest levels (unlike gecko setae). (C) The frictional adhesion model has an upper shear force limit. In comparison, the JKR model shows the typical behavior of an isotropic elastic material with adhesion.

relationship between the contact area and the normal force for a frictionless contact. To generate the curve in Fig. 10, the contact area was first calculated as a function of normal force, and then, a uniform shear strength was assumed across the contact area in order to arrive at a shear force limit, essentially relaxing the frictionless requirement after determining the contact area. While this may be a rough approximation, it is able to provide a qualitative picture of the forces that can be sustained by contacts fitting the JKR model. The frictional adhesion model has been scaled to fit the data from the DPS patches, and the JKR model has been scaled for comparison purposes. Mathematically, the frictional adhesion model is given by

$$F_N \geq -\frac{1}{\mu} F_T \quad \left\{ \begin{array}{l} F_T < 0 \\ F_N \geq -\tan(\alpha^*) F_T \quad \left\{ \begin{array}{l} 0 \leq F_T \leq F_{\max} \end{array} \right. \end{array} \right. \quad (7)$$

where  $\alpha^*$  is the critical angle [4],  $\mu$  is the coefficient of friction,  $F_T$  is the tangential (shear) load, taken positive when pulling in the adhesive direction, and  $F_N$  is the normal force, taken positive when compressive. The limit  $F_{\max}$  is a function of the maximum shear load that a gecko or robot can apply, the material strength, and the shear strength of the contact interface. Equation (7) shows how the maximum adhesion is directly related to the amount of the tangential force present.

The curves in Fig. 10 are the respective 2-D limit curves for the contact, i.e., the limiting combinations of normal and tangential force that will cause the contact to fail. The DPS show behavior similar to the frictional adhesion model for the gecko, and are clearly anisotropic with respect to adhesion. The DPS data also resemble data that would be obtained for peeling a sticky, elastic tape as described in the Kendall peel model [19]. In this case, although the toe patches are not peeled like a tape from one edge, the individual stalk tips do peel like tape of tapering thickness. However, the behavior of the DPS arrays at

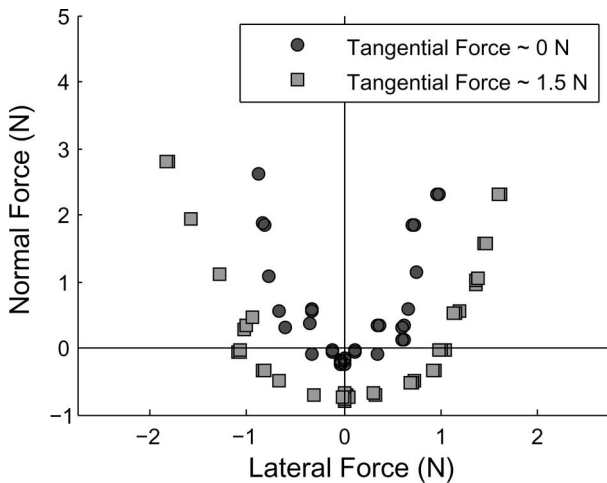


Fig. 11. Pull-off data for the DPS patches in the normal lateral plane. Data are shown for two different levels of tangential force, approximately 0 and 1.5 N.

the origin (approaching zero tangential force and normal force) is closer to that of the frictional adhesion model than the Kendall tape peeling model.

Fig. 11 shows the corresponding pull-off force data for the DPS in the normal lateral plane. Not surprisingly, the DPS show symmetric behavior when pulled in the positive or negative lateral direction. The amount of adhesion depends on the amount of tangential loading that is also present. Taken together, the two data sets in Figs. 10 and 11 represent slices of a convex 3-D limit surface in force space. Forces within the limit surface are safe; forces outside the surface will cause failure through sliding or detachment.

A consequence of the directional behavior of the DPS array is that the amount of adhesion can be controlled by changing the tangential force. To increase the available adhesion, the robot can pull harder in the tangential direction. Conversely, to facilitate smooth detachment, the robot can unload the foot in the tangential direction, approaching the origin in Fig. 10. In contrast, an isotropic elastic material described by the JKR model is difficult to detach smoothly because maximum adhesion is present when the tangential force is zero.

More generally, the directional adhesion in geckos and Stickbot requires different force control strategies than isotropic adhesion. A simple 2-D model can be used to illustrate the difference. Fig. 12 shows schematically the optimal tangential forces at the front and rear feet of a planar gecko or robot perched on surfaces of various inclinations. There are three equilibrium equations in the plane and four unknowns, corresponding to the magnitudes of the normal and tangential forces at each foot. The remaining DOFs is the magnitude of the internal (compressive or tensile) force, parallel to the surface, between the front and rear feet:  $F_{\text{Int}} = F_{T1} - F_{T2}$ . The internal force can be adjusted to keep each contact within its corresponding limit surface. Let  $\mathbf{F}_i = [F_{Ti}, F_{Ni}]$  be the contact force at the  $i$ th foot. The contact model can be defined by a parametric convex curve  $\mathbf{R}(x, y)$ , with points  $\mathbf{F} = [F_T, F_N]$  lying inside the curve being stable contacts. The distance any particular foot is from

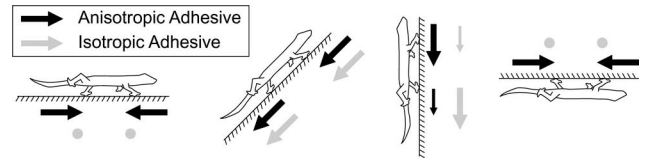


Fig. 12. Schematic of optimal tangential forces for a planar two-legged climber under isotropic versus anisotropic adhesion at different inclinations. Arrow directions and magnitudes shown in proportion to optimal tangential forces (dot represents zero tangential force).

violating a contact constraint is then

$$d_i = \min_{x,y} (\|\mathbf{F}_i - \mathbf{R}(x, y)\|). \quad (8)$$

For a model with two feet in contact with the surface, the overall stability margin becomes  $d = \min(d_1, d_2)$ , where  $d_1$  represents the front foot and  $d_2$  represents the rear foot.

Results of optimizing stability for the planar model using both the contact models given in Fig. 10 are given in Fig. 12. On vertical surfaces, the front foot must generate adhesion to prevent pitch back. The anisotropic model predicts that the front foot should bear more of the weight, since increasing tangential force increases available adhesion. The opposite is true for the isotropic model, namely that the rear foot should bear more weight because tangential forces on the front foot decrease adhesion. On inverted surfaces, the isotropic model predicts zero tangential forces since gravity is pulling along the normal, maximizing adhesion. Alternatively, the anisotropic model cannot generate adhesion without tangential forces, and in this case, the rear foot must be reversed and both feet must pull inward to generate tangential forces that will produce enough adhesion for stability. Interestingly, the anisotropic model also predicts that the same foot reversal strategy is optimal on the level ground, which would increase the maximum perturbation force that could be withstood. The predictions of the anisotropic model qualitatively match observations of geckos running on walls and ceilings, and reorienting their feet as they climb in different directions [5].

#### IV. DISTRIBUTED FORCE CONTROL

##### A. Distributed Force Control in the Gecko

As the previous section suggests, unlike a walking or running quadruped, a climbing gecko or robot must pay continuous attention to the control of internal forces whenever its feet are in contact with the climbing surface. In the gecko, it has been observed that even at speeds of over 1 m/s, attachment and lift-off are smooth, low-force events [5]. The gecko does not need to produce decelerating contact forces while climbing, but it does need to adjust the orientation of its feet as it maneuvers, to ensure that toes are always loaded in the proper direction for adhesion. On overhanging surfaces, the body-oriented lateral forces are high, as one would expect, and directed inward toward the center of mass. Geckos can also use their tails to affect the dynamic force balance. If the front feet lose their grip, the tail immediately presses against the wall and the rear legs provide the necessary pull-in force [5].

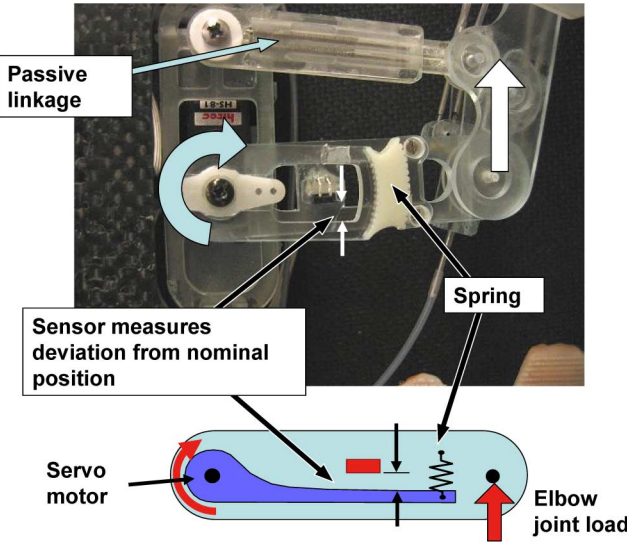


Fig. 13. Tangential force sensor measuring deviation of serial compliance at shoulder joint.

### B. Distributed Force Control in Stickybot

To achieve smooth engagement and disengagement and control of internal forces, Stickybot employs force feedback in the tangential (fore-aft) direction, coupled with a grasp-space stiffness controller. The control is implemented in hardware using a single master microcontroller (PIC18F4520) and four slave microcontrollers (PIC12F683) connected using an I<sup>2</sup>C bus. The master microcontroller runs the control code and outputs the 12 pulse-width-modulated signals to independently control each of Stickybot's servos (two servos for each leg and an additional servo for flexing the toes). Each slave microcontroller reads and digitizes the analog force sensor data from a single leg, and transmits that digital data to the master over the I<sup>2</sup>C bus.

### C. Force Sensors

Stickybot's force sensors are located on its shoulder joints (Fig. 13), and measure the deflection of an elastomeric spring via a ratiometric Hall effect sensor (Honeywell: SS495A). The Hall effect sensor outputs an analog voltage as a function of its position between two antialigned magnets. This analog voltage is digitized and run through a software low-pass filter at 50 Hz.

The mapping from the tangential force to the sensor output is affected by the nonlinearity of the viscoelastic spring and the Hall effect sensors' output as a function of displacement. In addition, as Stickybot's limbs rotate, both tangential and lateral forces can contribute to the displacement in the compliant element. However, due to the computation and space limitations of Stickybot's master microcontroller, the control law simply models the mapping as a linearization about zero force and zero displacement. Fig. 14 provides a comparison of the tangential force sensor output with the tangential and lateral contact forces for two successive contact periods, as measured by a vertical force plate mounted to the same six-axis load cell used in the previously described pull-off experiments. The figure shows that the tangential force sensor tracks the tangential forces relatively

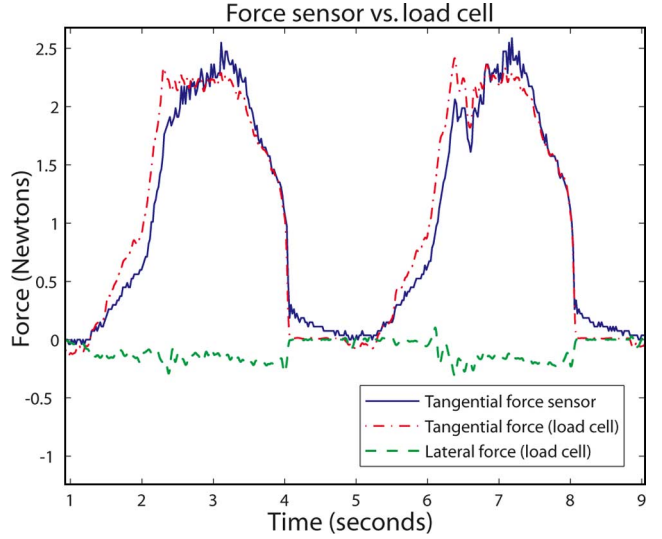


Fig. 14. Unfiltered tangential force sensor readings compared to tangential and lateral forces measured using a force plate mounted to a load cell.

closely, and that the lateral forces are small because, unlike the gecko, Stickybot cannot reorient its feet.

### D. Force Controller

When multiple limbs are in contact with the climbing surface, Stickybot's controller must consider how to coordinate them while continuing its vertical motion. This presents two different and sometimes contradictory goals: force balancing and leg positioning. In order to handle this tradeoff, Stickybot's controller implements a grasp-space stiffness controller [20]. Since Stickybot uses servomotors that only accept position commands, the stiffness control law is given as

$$\mathbf{y}_{\text{cmd}}(t) = \mathbf{y}_{\text{ff}}(\phi(t)) + \mathbf{C}(\mathbf{f}_s(t) - \mathbf{f}_d(\phi(t))) \quad (9)$$

where  $\mathbf{y}_{\text{cmd}}$  is the vector of stroke servo commanded positions,  $\mathbf{y}_{\text{ff}}$  is the feedforward position command (open loop gait),  $\mathbf{C}$  is the compliance matrix,  $\mathbf{f}_s$  is the vector of force sensor readings,  $\mathbf{f}_d$  is the vector of desired tangential forces, and  $\phi(t)$  is a function that maps from continuous time into periodic gait phase. While a diagonal compliance matrix  $\mathbf{C}$  would result in independent leg control, during stance, it is defined as

$$\mathbf{C} = \mathbf{G}^{-1} \mathbf{C}_0 \mathbf{G} \quad (10)$$

where  $\mathbf{C}_0 \neq \mathbf{I}$  is a diagonal gain matrix and  $\mathbf{G}$  is the grasp matrix given as

$$\mathbf{G} = \frac{1}{2} \begin{bmatrix} 1 & 1 & 1 & 1 \\ 1 & -1 & 1 & -1 \\ 1 & 1 & -1 & -1 \\ 1 & -1 & -1 & 1 \end{bmatrix}. \quad (11)$$

The grasp matrix comprises of four independent "grasp modes," or ways to linearly combine the force sensor data. The first row in  $\mathbf{G}$  corresponds to summing the tangential forces (Fig. 15). The second row corresponds to a measure of the sum of moments about the center of mass (the difference between total tangential force on the left and right limbs). The third and

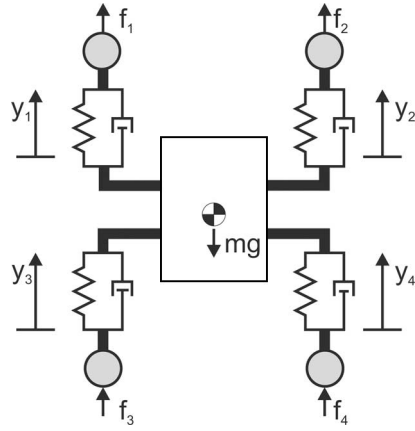


Fig. 15. Schematic used to generate values for the grasp matrix.

TABLE I  
PHYSICAL PARAMETERS FOR STICKYBOT

Body size	600 x 200 x 60 mm (excluding cables)
Body mass	370 g (including batteries and servo circuitry)
Maximum speed	4.0 cm/s (0.05 bodylengths/s)
Servo motors	Hitec HB65 x 8 Hs81 x 4
Batteries	lithium polymer x2 (3.7 V, 480 mAh per pack)

fourth rows are chosen such that  $G$  is orthogonal, thereby leaving four independent modes of control. The chosen values for those rows correspond to fore aft and diagonal coupling of the limbs, respectively. The implementation of stiffness control in grasp space creates a framework for force distribution. By increasing the compliances of all but the total tangential mode, the robot will evenly distribute the forces between the feet, and achieve force balance while remaining stiff to variations in loading.

## V. RESULTS

Stickybot is capable of climbing a variety of surfaces at 90° including glass, glossy ceramic tile, acrylic, and polished granite at speeds up to 4.0 cm/s (0.12 bodylengths/s, excluding the tail). The maximum speed of Stickybot on level ground is 24 cm/s and is limited by the speed of its actuators (Table I).

Fig. 16 presents typical force plate data of Stickybot climbing vertical glass. The left side shows data from the rear left foot and the right side displays data from the front right foot. Forces are in newtons and time in seconds. Data from two successive runs are shown to give an indication of the repeatability.

Section A in Fig. 16 (0–1.5 s) represents the preloading and flexing of the foot. There is almost no force in the lateral ( $X$ ) direction during preload. The tangential force ( $-Y$ ) is increasing. Although each foot would ideally engage with negligible normal force, there is a small amount of positive normal force during engagement. Weight transfer between diagonal pairs also occurs during section A.

Section B in Fig. 16 represents the ground stroke phase. There are equal and opposite forces in the  $X$ -direction for the front right and rear left feet, indicating that the legs are pulling in toward the body. This helps stabilize the body and is similar to the lateral forces exhibited in geckos (and in contrast to the outward lateral forces observed in small running animals such as

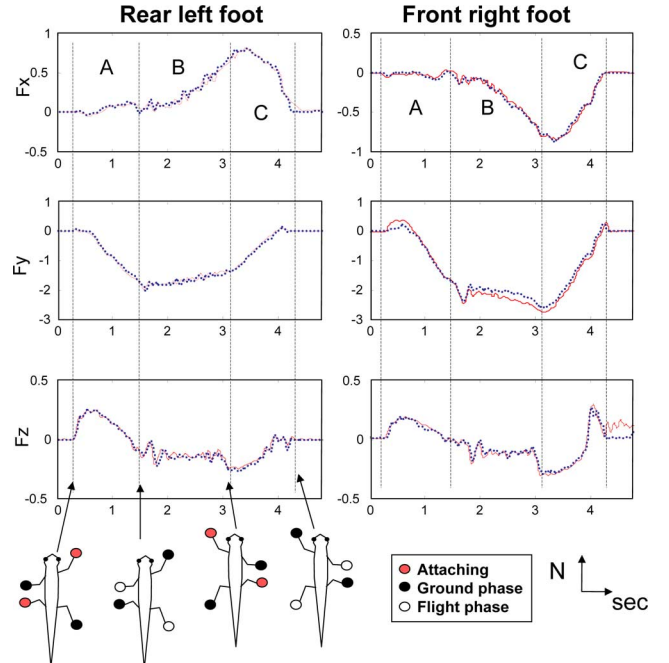


Fig. 16. Force plate data of rear left foot (left) and front right foot (right) of Stickybot climbing with a 6 s period at a speed of 1.5 cm/s. Data filtered at 10 Hz. Two successive runs are shown to illustrate repeatability.

lizards and insects) [5]. The  $Y$ -direction shows relatively steady tangential force, and the  $Z$ -direction indicates adhesion on both the front and rear feet. Note that this differs from gecko data, in which the rear feet exhibit positive normal force [5]. This is due to the fact that Stickybot uses its tail to prevent the body from pitching back, and geckos usually use their rear feet.

In Section C in Fig. 16, Stickybot releases the feet both by reducing the tangential force ( $Y$ ) and by peeling (utilizing digital hyperextension). Both the front and rear feet exhibit low detachment forces in the  $Z$ -direction, especially the rear foot. We note also that the transition between B and C is accompanied by a temporary increase in adhesion ( $-Z$  force) and subsequent decrease as the opposite diagonal feet come into engagement.

Fig. 17 shows a comparison of the force data for climbing with directional versus isotropic adhesive elastomeric pads. In this test, the isotropic pads were composed of arrays of pillars connected by a thin outer membrane of soft polyurethane (innovative polymers: 20 Shore-A hardness) to increase the contact area on smooth surfaces. The data for three successive cycles are shown to give an estimate of cycle to cycle variability. In each case, the robot cycled a single leg through an attach/load/detach cycle using the same six-axis load cell as in the previous tests. The other three limbs remained attached to the wall. As the plots show, the isotropic patches required a somewhat larger normal force (A) to produce comparable amounts of combined tangential force and adhesion for climbing (B). The unloading step for the anisotropic patches (C) is accomplished rapidly and results in negligible detachment force as the leg is removed. In contrast, the isotropic patch requires a longer peeling phase (C) and produces a very large pull-off force as the leg is withdrawn. This large detachment force was the main limitation of

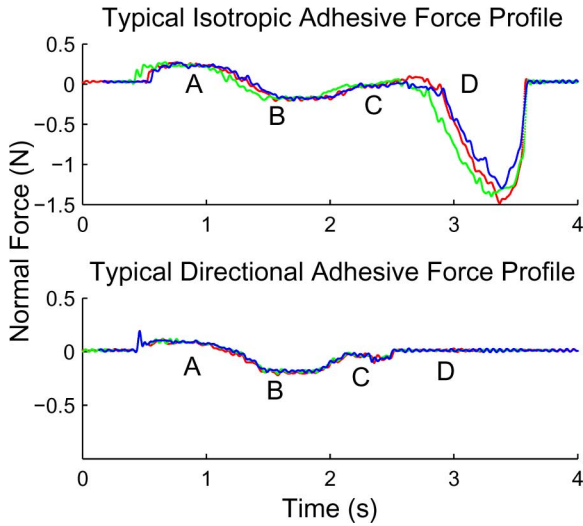


Fig. 17. Comparison of normal force profiles of anisotropic and isotropic patches on a climbing robot. Point A on the curves refers to the preloading phase of the cycle. Point B highlights when the foot is in the adhesive regime during a stroke. Points C and D are when the foot is unloaded and detached, causing large normal forces in the case of the isotropic patch.

the isotropic patches, producing perturbations that frequently caused the other feet to slip.

## VI. CONCLUSION AND FUTURE WORK

Taking cues from geckos, Stickybot uses three main principles to climb smooth surfaces. First, it employs *hierarchical compliance* that conforms at levels ranging from the micrometer to centimeter scale. Second, Stickybot takes advantage of *directional adhesion* that allows it to smoothly engage and disengage from the surface by controlling the tangential force. This prevents large disengagement forces from propagating throughout the body and allows the feet to adhere themselves to surfaces when loaded in shear. Interestingly, the motion strategy for engaging adhesives is similar to that used for microspines [2]. Third, Stickybot employs *force control* that works in conjunction with the body compliance and directional adhesive patches to control the tangential forces in the feet.

Some of the Stickybot's directional adhesive patches have been in continuous use for over six months without significant loss in performance; however, because the DPSs are made from a polyurethane that degrades with time, their sharp geometric features will eventually become dull and the patches will begin to lose some of their adhesive performance. As discussed in Section II, the DPSs use relatively large feature sizes and a soft material, and therefore, require periodic cleaning with a lint roller to maintain enough performance to allow Stickybot to climb well. Another limitation is that the stalk tips can fold on themselves; however, in this case, they can be reconditioned via a more thorough cleaning with soap and water.

The introduction of better adhesive structures with improved hierarchical compliances will allow Stickybot to climb rougher surfaces and yield longer climbs with an increased resistance to becoming dirty. The first priority is to create DPS arrays of smaller stalks and a correspondingly stiffer, more durable, and

dirt-resistant grade of polymer. Other improvements include improved force control and more attention to the gait and control of internal forces. Additional sensors in the feet should allow the robot to detect when good or poor contact has been made, which will improve the reliability of climbing on varying surfaces. Additional DOFs in the body should allow the robot to master vertical–horizontal transitions and other discontinuities. Once the climbing technology is understood, the ability to climb smooth surfaces will be integrated into the RiSE family of robots in an attempt to design a machine capable of climbing a wide variety of man-made and natural surfaces using a combination of adhesion and microspines [29].

## ACKNOWLEDGMENT

The authors thank J. Karpick, S. Dastoor, A. Parness, and A. McClung for their help in circuit board fabrication, coding, and gait generation in support of Stickybot.

## REFERENCES

- [1] E. Arzt, S. Gorb, and R. Spolenak, "From micro to nano contacts in biological attachment devices," *Proc. Natl. Acad. Sci. USA*, vol. 100, no. 9, pp. 10603–10606, 2003.
- [2] A. T. Asbeck, S. Kim, M. R. Cutkosky, W. R. Provancher, and M. Lanzetta, "Scaling hard vertical surfaces with compliant microspine arrays," *Int. J. Rob. Res.*, vol. 25, no. 12, pp. 1165–1179, 2006.
- [3] K. Autumn, *Biological Adhesives*, vol. XVII. Berlin, Germany: Springer-Verlag, 2006.
- [4] K. Autumn, A. Dittmore, D. Santos, M. Spenko, and M. Cutkosky, "Frictional adhesion: A new angle on gecko attachment," *J. Exp. Biol.*, vol. 209, no. 18, pp. 3569–3579, 2006.
- [5] K. Autumn, S. T. Hsieh, D. M. Dudek, J. Chen, C. Chitaphan, and R. J. Full, "Dynamics of geckos running vertically," *J. Exp. Biol.*, vol. 209, no. 2, pp. 260–272, 2006.
- [6] K. Autumn, C. Majidi, R. E. Groff, A. Dittmore, and R. Fearing, "Effective elastic modulus of isolated gecko setal arrays," *J. Exp. Biol.*, vol. 209, pp. 3558–3568, 2006.
- [7] K. Autumn, M. Sitti, Y. Liang, A. Peattie, W. Hansen, S. Sponberg, T. Kenny, R. Fearing, J. Israelachvili, and R. Full, "Evidence for van der waals adhesion in gecko setae," *Proc. Natl. Acad. Sci. U S A*, vol. 99, no. 19, pp. 12252–12256, 2002.
- [8] C. Balaguer, A. Gimenez, J. Pastor, V. Padron, and C. Abderrahim, "A climbing autonomous robot for inspection applications in 3D complex environments," *Robotica*, vol. 18, no. 3, pp. 287–297, 2000.
- [9] M. Binnard and M. Cutkosky, "A design by composition approach for layered manufacturing," *ASME J. Mech. Des.*, vol. 122, no. 1, pp. 91–101, 2000.
- [10] B. Chan, N. J. Balmforth, and A. E. Hosoi, "Building a better snail: Lubrication and gastropod locomotion," *Phys. Fluids*, vol. 17, 2005, CID 10 113101.
- [11] C. A. Dahlquist, "Pressure-sensitive adhesives," in *Treatise on Adhesion and Adhesives*, vol. 2, R. L. Patrick, Ed. New York: Dekker, 1969, pp. 219–260.
- [12] K. Daltonio, S. Gorb, A. Peressadko, A. Horchler, R. Ritzmann, and R. Quinn, "A robot that climbs walls using micro-structured polymer feet," in *Proc. CLAWAR*, 2005, pp. 131–138.
- [13] K. Daltonio, A. Horchler, S. Gorb, R. Ritzmann, and R. Quinn, "A small wall-walking robot with compliant, adhesive feet," in *Proc. Int. Conf. Intell. Robots Syst.*, 2005, pp. 4018–4023.
- [14] H. Gao, X. Wang, H. Yao, S. Gorb, and E. Arzt, "Mechanics of hierarchical adhesion structures of geckos," *Mech. Mater.*, vol. 37, pp. 275–285, 2005.
- [15] H. Gao and H. Yao, "Shape insensitive optimal adhesion of nanoscale fibrillar structures," *Proc. Natl. Acad. Sci. U S A*, vol. 101, no. 21, pp. 7851–7856, 2004.
- [16] S. Gorb, M. Varenberg, A. Peressadko, and J. Tuma, "Biomimetic mushroom-shaped fibrillar adhesive microstructure," *J. Royal Soc. Interface*, vol. 4, no. 13, pp. 271–275, 2006.
- [17] J. Israelachvili, *Intermolecular and Surface Forces*. New York: Academic, 1992.

- [18] K. L. Johnson, K. Kendall, and A. D. Roberts, "Surface energy and the contact of elastic solids," in *Proc. Royal Soc. A: Math., Phys. Eng. Sci.*, 1971, vol. 324, no. 1558, pp. 301–313.
- [19] K. Kendall, "Thin-film peeling—The elastic term," *J. Phys. D: Appl. Phys.*, vol. 8, no. 13, pp. 1449–1452, 1975.
- [20] J. Kerr and B. Roth, "Analysis of multifingered hands," *Int. J. Robot. Res.*, vol. 4, no. 4, pp. 3–17, 1986.
- [21] D. S. Kim, H. S. Lee, J. Lee, S. Kim, K.-H. Lee, W. Moon, and T. H. Kwon, "Replication of high-aspect-ratio nanopillar array for biomimetic gecko foot-hair prototype by UV nano embossing with anodic aluminum oxide mold," *Microsyst. Technol.*, vol. 13, no. 5/6, pp. 601–606, 2007.
- [22] S. Kim and M. Sitti, "Biologically inspired polymer microfibers with spatulate tips as repeatable fibrillar adhesives," *Appl. Phys. Lett.*, vol. 89, pp. 261911-1–261911-3, 2006.
- [23] S. Kim, M. Spenko, S. Trujillo, B. Heyneman, V. Matolli, and M. Cutkosky, "Whole body adhesion: Hierarchical, directinoal and distributed control of adhesive forces for a climbing robot," presented at the IEEE ICRA, Rome, Italy, 2007, pp. 1268–1273.
- [24] G. La Rosa, M. Messina, G. Muscato, and R. Sinatra, "A low-cost lightweight climbing robot for the inspection of vertical surfaces," *Mechatronics*, vol. 12, no. 1, pp. 71–96, 2002.
- [25] M. Northern and K. Turner, "A batch fabricated biomimetic dry adhesive," *Nanotechnology*, vol. 16, pp. 1159–1166, 2005.
- [26] A. Peressadko and S. N. Gorb, "When less is more: Experimental evidence for tenacity enhancement by division of contact area," *J. Adhesion*, vol. 80, no. 4, pp. 247–261, 2004.
- [27] B. N. J. Persson and S. Gorb, "The effect of surface roughness on the adhesion of elastic plates with application to biological systems," *J. Chem. Phys.*, vol. 119, no. 21, pp. 11437–11444, 2003.
- [28] D. Santos, S. Kim, M. Spenko, A. Parness, and M. Cutkosky, "Directional adhesive structures for controlled climbing on smooth vertical surfaces," presented at the IEEE ICRA, Rome, Italy, 2007, pp. 1262–1267.
- [29] A. Saunders, D. Goldman, R. Full, and M. Buehler, "The rise climbing robot: Body and leg design," presented at the SPIE Unmanned Syst. Technol. VII, Orlando, FL, 2006, vol. 6230.
- [30] M. Sitti and R. Fearing, "Synthetic gecko foot-hair micro/nano-structures as dry adhesives," *Adhesion Sci. Technol.*, vol. 17, no. 8, pp. 1055–1073, 2003.
- [31] O. Unver, M. Murphy, and M. Sitti, "Geckobot and waalbot: Small-scale wall climbing robots," presented at the AIAA 5th Aviation Technol., Integr., Oper. Conf. Arlington, VA, 2005.
- [32] Vortex. (2006). [Online]. Available: [www.vortexhc.com](http://www.vortexhc.com)
- [33] L. E. Weiss, R. Merz, F. Prinz, G. Neplotnik, P. Padmanabhan, L. Schultz, and K. Ramaswami, "Shape deposition manufacturing of heterogenous structures," *J. Manuf. Syst.*, vol. 16, no. 4, pp. 239–248, 1997.
- [34] Z. Xu and P. Ma, "A wall-climbing robot for labeling scale of oil tank's volume," *Robotica*, vol. 20, no. 2, pp. 203–207, 2002.
- [35] H. Yao and H. Gao, "Mechanics of robust and releasable adhesions in biology: Bottom-up designed hierarchical structures of gecko," *J. Mech. Phys. Solids*, vol. 54, pp. 1120–1146, 2006.
- [36] B. Yurdumakan, R. Ravarikar, P. Ajayan, and A. Dhinojwala, "Synthetic gecko foot-hairs from multiwalled carbon nanotubes," *Chem. Commun.*, vol. 30, pp. 3799–3801, 2005.
- [37] Y. Zhao, T. Tong, L. Delzeit, A. Kashani, M. Meyyapan, and A. Majumdar, "Interfacial energy and strength of multiwalled-carbon-nanotube-based dry adhesive," *Vacuum Sci. Technol. B*, vol. 24, pp. 331–335, 2006.
- [38] J. Zhu, D. Sun, and S. K. Tso, "Development of a tracked climbing robot," *Intell. Robot. Syst.*, vol. 35, no. 4, pp. 427–444, 2002.



**Sangbae Kim** (S'06) received the B.S. degree in mechanical engineering from Yonsei University, Seoul, Korea, in 2001. He is currently working toward the Ph.D. degree in the Biomimetics Laboratory, Stanford University, Stanford, CA.

He was a Mechanical Designer at a 3-D scanner company. His current research interest include bioinspired flexible robot design and directional adhesion. His bioinspired climbing robot was selected as one of the best inventions in *Time Magazine* in 2006 and also featured in *Forbes Magazine*, "Modern Marvels" on the History Channel, and *Wired Science*.



**Matthew Spenko** (S'07–M'07) received the B.S. degree from the Northwestern University, Evanston, IL, in 1999, and the M.S. and Ph.D. degrees from Massachusetts Institute of Technology, Cambridge, in 2001 and 2005, respectively, all in mechanical engineering.

From 2005 to 2007, he was an Intelligence Community Postdoctoral Fellow at Stanford University, Stanford, CA. He is currently a Professor at Illinois Institute of Technology, Chicago. His current research interests include robotics with specific attention to designing, understanding, and exploiting the dynamics of mobile systems in the context of challenging environments.



**Salomon Trujilio** received the B.S. degree from California Institute of Technology, Pasadena, in 2004, and the M.S. degree in 2005 from Stanford University, Stanford, CA, where he is currently working toward the Ph.D. degree at the Biomimetics Dexterous Manipulation Laboratory, all in mechanical engineering. His current research interests include mechatronic systems, legged robotics, and control systems.



**Barrett Heyneman** received the B.S. degree from California Institute of Technology, Pasadena, and the M.S. degree from Stanford University, Stanford, CA both in mechanical engineering, in 2005 and 2007, respectively. He is currently working toward the Ph.D. degree at the Biomimetic and Dextrous Manipulation Laboratory, Department of Mechanical Engineering, Stanford University, Stanford, CA.

His current research interests include gait generation and regulation for legged robots, control schemes for underactuated and compliant systems, autonomous sensor calibration for mobile platforms, and machine learning for locomotion.



**Daniel Santos** (S'06) received the B.Sc. degree in mechanical and electrical engineering from Massachusetts Institute of Technology (MIT), Cambridge, in 2002, and the M.Sc. degree in mechanical engineering from Stanford University, Stanford, CA, in 2004, where he is currently working toward the Ph.D. degree.

His current research interests include legged robots, mechatronics, and controls.



**Mark R. Cutkosky** (M'92) received the Ph.D. degree in mechanical engineering from Carnegie Mellon University, Pittsburgh, PA, in 1985.

In 1985, he joined Stanford University, Stanford, CA, where he is currently a Professor at the Center for Design Research, Department of Mechanical Engineering. He was with the Robotics Institute at Carnegie Mellon University and a Machine Design Engineer at ALCOA, Pittsburgh. He has graduated 29 Ph.D. students and published extensively in these areas. He has consulted with various companies on robotics and human/computer interaction devices and holds several patents on related technologies. His current research interests include robotic manipulation and tactile sensing, mechatronic systems design, and the design and fabrication of biologically inspired robots.

Dr. Cutkosky was the recipient of the Fulbright Faculty Chair, Charles M. Pigott Professorship at Stanford University, and the NSF Presidential Young Investigator award. He is a member of the American Society of Mechanical Engineers (ASME) and Sigma Xi. His work on bioinspired climbing and running robots has been featured in *Discover Magazine*, *The New York Times*, *Metropolis Magazine*, and other publications and has appeared on the CBS Evening News, Next @CNN, Science Central News, Quantum, and other popular media.